nature cell biology

DOI: 10.1038/ncb1991

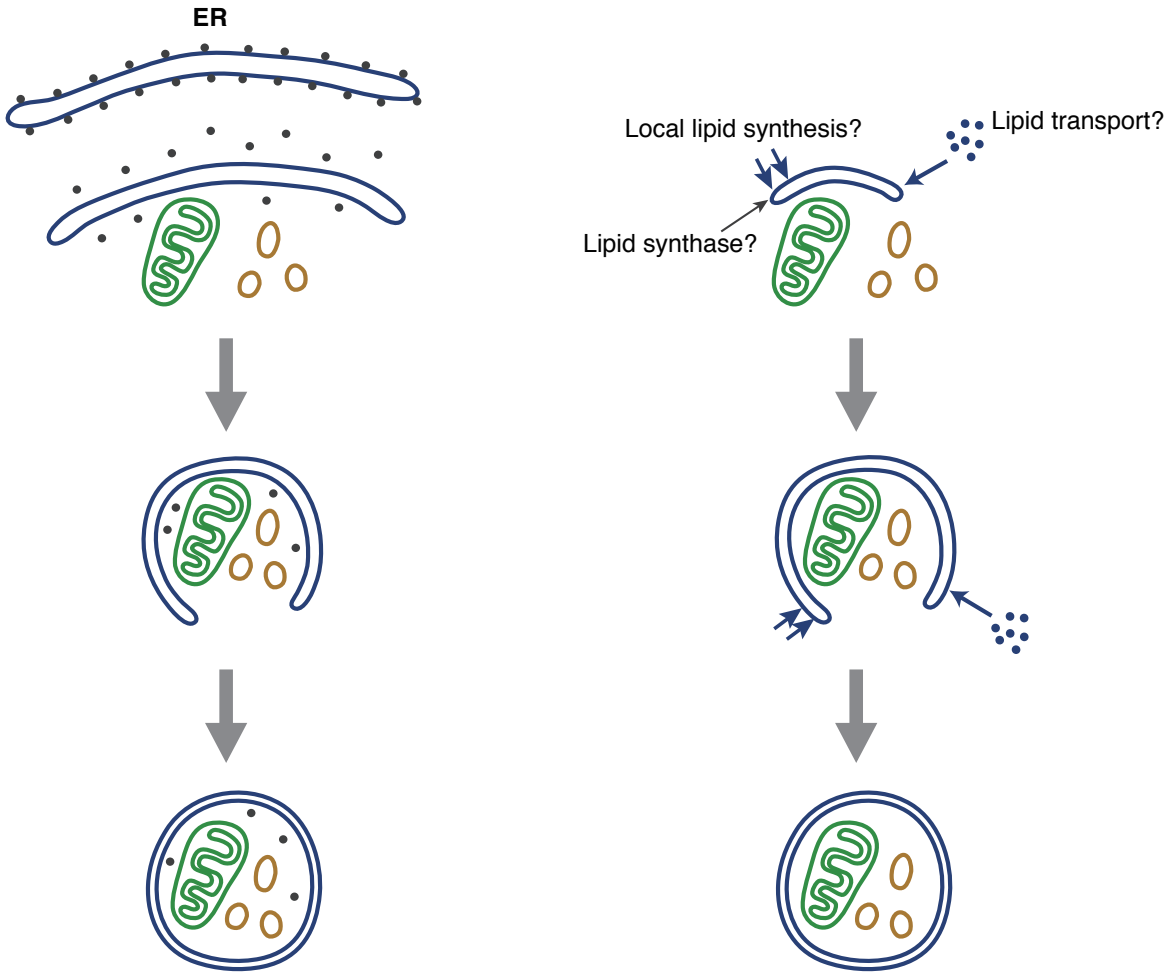

Model 1.

Direct maturation from the ER.

Model 2.

Localized lipid synthesis or transport.

Figure S1 Two proposed models for autophagosome formation. Based on previous studies, it has been suggested that autophagosomes are formed either by direct maturation from the ER, or by de novo membrane formation by localized lipid synthesis or transport[5, 9].

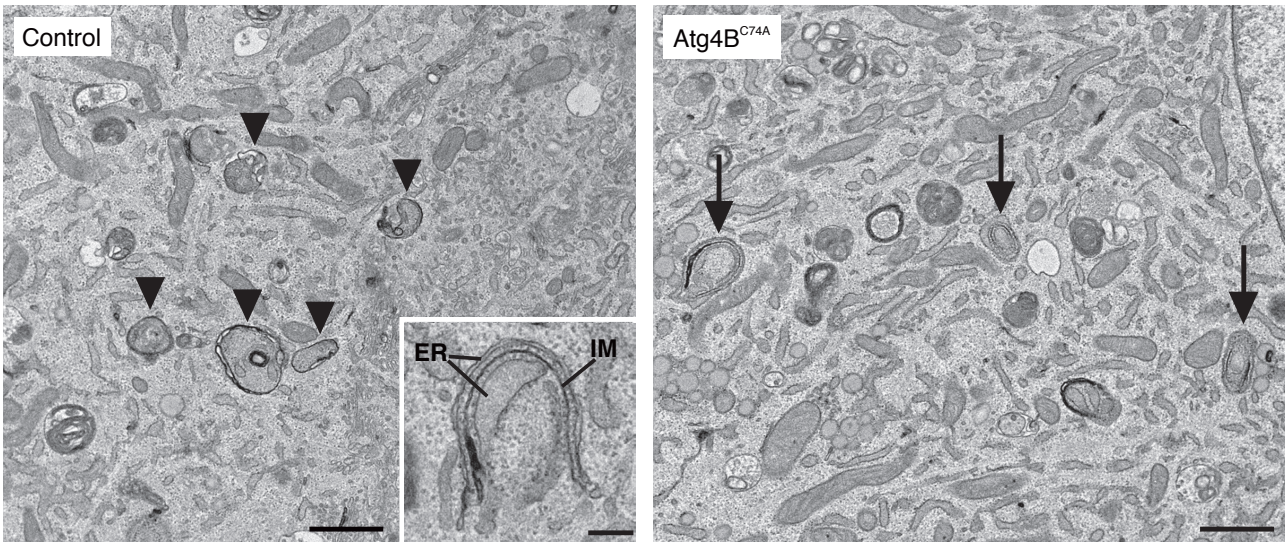

Figure S2 Electron micrographs of NIH3T3 cells stably expressing either empty vector (Control) or the Atg4B^{C74A} mutant cultured in nutrient free medium for 1h. Autophagosomes (arrowheads) were observed in control cells, while IMs (arrows) were more evident in Atg4B^{C74A} expressing cells. The inset shows a representative image of IMs observed in control cells. Scale bar, 1 μm and 200 nm in the inset.

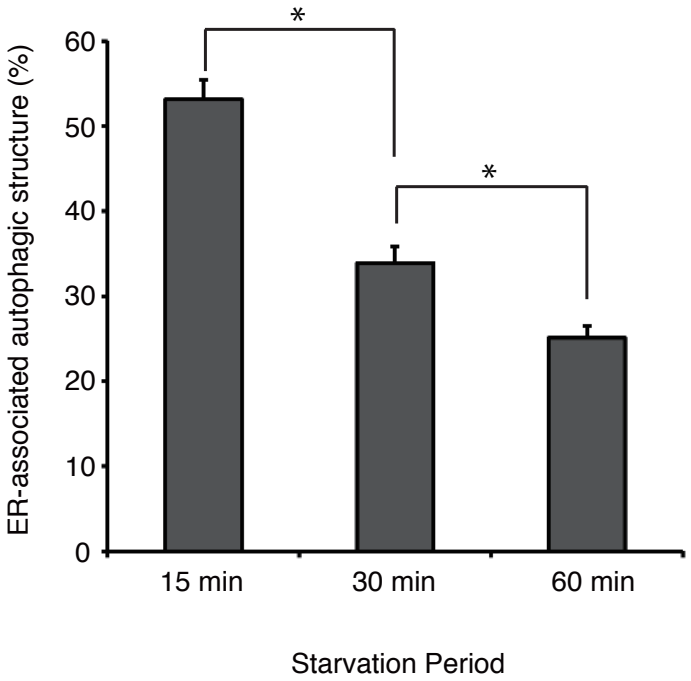

Figure S3 The ratio of ER-associated autophagic structures (ER-IM complexes) to total autophagic structures. MEF cells were incubated in nutrient free medium for the indicated time periods, then fixed and processed for EM analysis. Autophagic structures were collected from 1088 cells starved for 15 min., 494 cells starved for 30 min., and 283 cells starved for 60 min. The number of autophagic structures collected at each time point was 145, 230, and 320. Data are expressed as means ± SD of triplicates from representative experiments. *P < 0.01.

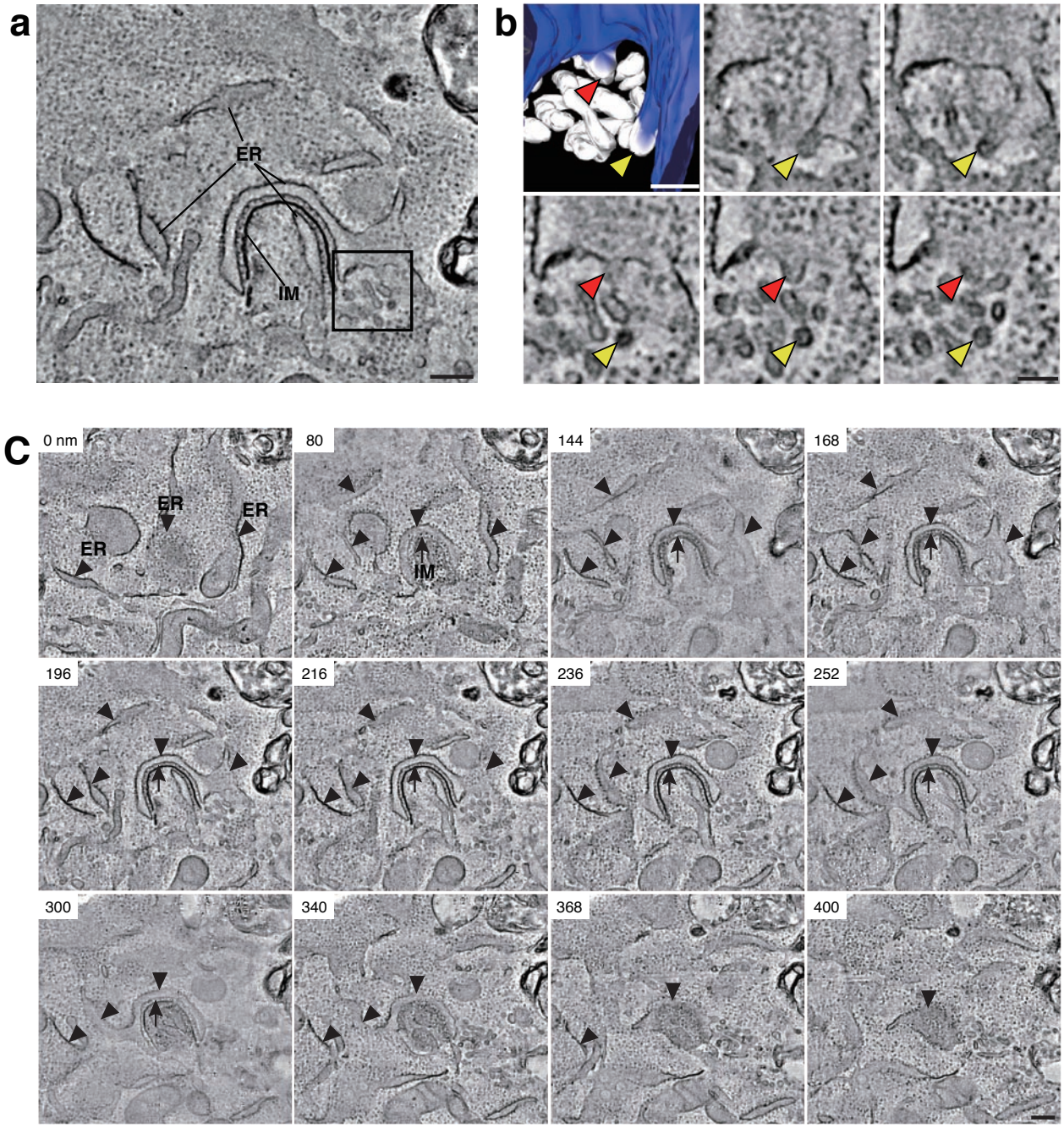

Figure S4 Electron tomography of the ER-IM complex. (**a**) A 4 nm tomographic slice of an area containing an ER-IM complex. (**b**) A 3-D model and tomographic slices (12 nm intervals) of the boxed region in (a) depict the continuity of VTC with the ER (red and yellow arrowheads). (**c**) A panel of tomographic slices (also depicted in Movie 1) showing that the ER-IM complex forms from a subdomain of the ER. Numbers indicate the depth of the tomographic slices. The size of this particular reconstructed structure was estimated to be about $1.8 \times 1.5 \times 0.4\ \mu m^3$. Arrows and arrowheads indicate the IM and the ER, respectively. Scale bar, 200 nm in (**a**) and (c), 100 nm in (**b**).

Supplementary movie legends

Movie 1 This movie depicts serial tomographic slices of an area containing an ER-IM complex (one of the slices is depicted in Fig. S4) generated from three 200 nm thick sections, showing that the ER-IM complex forms from a subdomain of the ER.

Movie 2 Rotating view of the ER-IM complex presented in Fig. 3b showing the IM sandwiched between two ER cisternae.

Movie 3 This movie depicts serial tomographic slices (one of the slices is depicted in Fig. 3) of a portion of the ER-IM complex, revealing the continuity of the IM with the ER. The arrowhead indicates the edge of the IM connected to the ER.

Movie 4 This movie depicts a rotating view of the connection between the IM and the associated ER presented in Fig. 3c and 3d.

Movies 5 and **6**. These movies show rotating views of the connection between IMs and the ER from two different ER-IM complexes presented in Figure 4.